Earth and Planetary Science Letters, 113 (1992) 251–266
Elsevier Science Publishers B.V., Amsterdam

[DT]

Evolution of terrestrial proto-CO_2 atmosphere coupled with thermal history of the earth

Eiichi Tajika and Takafumi Matsui

Department of Earth and Planetary Physics, Faculty of Science, University of Tokyo, Tokyo 113, Japan

Received June 3, 1991; revision accepted June 17, 1992

ABSTRACT

The effect of volatile exchange between surface reservoirs and the mantle on the evolution of proto-CO_2 atmosphere on the Earth is investigated using a global carbon cycle model coupled with thermal evolution of the mantle. Carbon is assumed to circulate among five reservoirs (atmosphere, ocean, continents, seafloor and mantle) and the carbon flux of each reservoir is calculated under varying conditions, such as an increase in solar luminosity, continental growth, and a decrease in tectonic activity with time. We consider processes such as continental weathering, carbonate precipitation in the ocean, carbonate accretion to the continents, metamorphism of carbonates followed by CO_2 degassing through arc volcanism, carbon regassing into the mantle, and CO_2 degassing from the mantle. The degassing rate of volatiles from the mantle is assumed to be proportional to the volatile concentration in the mantle multiplied by the mantle degassing volume The mantle degassing volume is determined by the seafloor spreading rate and the melt generation depth in the mantle. We use a parameterized convection model to calculate the thermal evolution of the mantle, from which we estimate the seafloor spreading rate and the melt generation depth in the mantle.

Numerical simulations suggest that the amount of surface carbon at the present time would be in a steady state This is because the response time of the carbon cycle system against the perturbation for surface carbon is short, being estimated at about 900 million years under the present conditions Thus the present amount of surface carbon would not be affected by the initial amount of surface carbon The seafloor spreading rate would have been almost constant throughout the Earth's history to explain apparent constancy of the carbon isotope ratio in the mantle after about 3.5 billion years ago. The surface carbon might probably have been circulated between surface reservoirs and the mantle once or twice after the Archean period In any event, CO_2 in the proto-atmosphere on the Earth is suggested to have decreased with the growth of continents, resulting in stabilization of the terrestrial environment against the increase in solar luminosity

1. Introduction

A steam atmosphere was probably formed by impact degassing during accretion of the Earth and the surface of accreting Earth was covered with a magma ocean owing to the blanketing effect of this atmosphere [1–4]. At the end of accretion, the steam atmosphere became unstable with a decrease in impact energy flux and thus H_2O in the proto-atmosphere condensed to form the proto-oceans [5,6]. The atmosphere just after the formation of the proto-ocean was considered to be composed mainly of CO_2 because carbon would be the second most abundant volatile element in the accreting material, judging from the composition of chondrite meteorites [e.g., 7]. CO_2 is a greenhouse gas. Hence, the variation of CO_2 content in the atmosphere affects the surface temperature [8–11]. This indicates a potential importance of the CO_2 cycle among surface reservoirs in the evolution of the terrestrial surface environment, because the luminosity of the sun increased to its present level from a value that was 30% lower during the history of the Earth [12–15]. Therefore, as suggested in our

Correspondence to. Eiichi Tajika, Department of Earth and Planetary Physics, Faculty of Science, University of Tokyo, Tokyo 113, Japan.

previous paper [16], the evolution of proto-CO_2 atmosphere plays a dominant role in the evolution of the terrestrial environment.

The amount of CO_2 in the atmosphere is regulated through the carbon cycle among the surface carbon reservoirs, such as the atmosphere, ocean and crust, and the interior of the Earth [16–19]. We recently investigated the effect of the carbon cycle on the terrestrial environment over the entire history of the Earth. We proposed that the CO_2 in the proto-atmosphere has decreased with growth of the continents, resulting in stabilization of the terrestrial environment [16]. This is because the continents supply a large quantity of cations to the oceans through weathering, followed by precipitation of more carbonate on the seafloor; this finally results in consumption of atmospheric CO_2. Because some seafloor carbonates accrete to the continents, the latter also act as a large sink for surface carbon. This means a decrease in the amount of carbon circulating within the surface layers because continental carbon has a very long residence time in the carbon cycle. As a consequence, CO_2 in the atmosphere reaches its present lower level ($\sim 10^{-4}$ bar) and this provides a mechanism that stabilizes the terrestrial environment against the increase in solar luminosity [16].

We ignored the role of the mantle in the evolution of the terrestrial environment in our previous paper. However, the mantle is considered to be another sink and source candidate for the surface carbon through the volatile exchange between the surface and the mantle. Degassing and regassing rates of volatile elements are probably dependent on the tectonic activity [20,21]. In our previous study, tectonic activity, such as the seafloor spreading rate, was simply considered to be proportional to the mantle heat flow, which is assumed to be proportional to the radiogenic heat production rate [16]. This is obviously too simple for discussing a degassing history because the mantle heat flow is actually related to the efficiency of mantle convection. In this study, we thus investigate the evolution of proto-CO_2 atmosphere using a global carbon cycle model coupled with the thermal history of the Earth.

2. Carbon cycle model

The carbon cycle was described in detail in our previous paper [16], and has also been discussed by various other authors [e.g., 17–19]. We shall, however, briefly present the carbon cycle here (Fig. 1).

CO_2 in the atmosphere dissolves into raindrops or groundwater and produces carbonic acid, which weathers the silicate and carbonate minerals on the land surface. Weathering reactions are expressed as follows:

$$2CO_2 + CaSiO_3 + H_2O \rightarrow Ca^{2+} + 2HCO_3^- + SiO_2 \quad (1)$$

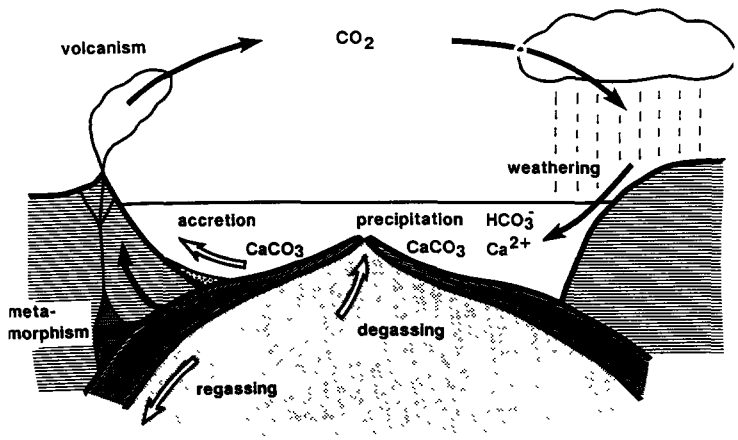

Fig. 1. Schematic diagram of the global carbon cycle on the Earth. The black arrows represent the processes associated with the carbonate–silicate geochemical cycle [17–19]. The white arrows represent the additional processes comprising the global carbon cycle during the evolution of the Earth [16].

$$2CO_2 + MgSiO_3 + H_2O \rightarrow Mg^{2+} + 2HCO_3^- + SiO_2 \quad (2)$$

$$CO_2 + CaCO_3 + H_2O \rightarrow Ca^{2+} + 2HCO_3^- \quad (3)$$

$$CO_2 + MgCO_3 + H_2O \rightarrow Mg^{2+} + 2HCO_3^- \quad (4)$$

These are just shown as typical expressions for silicate and carbonate weathering. We consider calcite and magnesite as carbonates, but here, for simplicity, not dolomite [16].

Bicarbonate ions and cations produced by the weathering are carried to the oceans by rivers and will react again with each other to form carbonates, as follows:

$$Ca^{2+} + CO_3^{2-} \rightarrow CaCO_3 \quad (5)$$

$$Mg^{2+} + CO_3^{2-} \rightarrow MgCO_3 \quad (6)$$

This process is almost completely promoted by organic activity at present [e.g., 22]. It could, however, be conducted inorganically. The carbonates are deposited on the seafloor, where they move with the motion of the oceanic plates, and eventually reach the subduction zone. Some carbonates are metamorphosed under certain conditions of temperature and pressure, as follows:

$$CaCO_3 + SiO_2 \rightarrow CaSiO_3 + CO_2 \quad (7)$$

$$MgCO_3 + SiO_2 \rightarrow MgSiO_3 + CO_2. \quad (8)$$

CO_2 is reproduced by this process and returns to the atmosphere through arc volcanism. This is the so-called "carbonate–silicate geochemical cycle" [17–19]. In addition to these processes, some carbonates at the subduction zone will be accreted to the continental crust in the form of accretionary prisms (or, alternatively, carbonates may also be precipitated directly onto the continental shelves), and other carbonates will be subducted into the mantle with the descending slab. Carbon in the mantle degasses at the mid-ocean ridge through plate formation. In this way, carbon circulates among the surface reservoirs and the interior throughout the history of the Earth. We call this "the global carbon cycle". For simplicity, in this study we do not consider ordinary metamorphic reactions through which CO_2 might return to the atmosphere. Neither do we take into account an organic carbon cycle, because only 20% of the total amount of surface carbon is involved in the organic carbon cycle [e.g., 23].

For modeling the global carbon cycle, we assumed five carbon reservoirs (the atmosphere, the ocean, the continents, the seafloor and the mantle) and calculated carbon fluxes under varying conditions, such as increase in solar luminosity, continental growth, and decrease in tectonic activities such as the seafloor spreading rate [16]. The mass balance equations among the carbon reservoirs are given, as follows:

$$\frac{dL_{cc}}{dt} = F_A^{cc} - F_W^{cc} \quad (9)$$

$$\frac{dL_{mc}}{dt} = F_A^{mc} - F_W^{mc} \quad (10)$$

$$\frac{dP_{cc}}{dt} = F_P^{cc} - F_A^{cc} - F_M^{cc} - F_R^{cc} \quad (11)$$

$$\frac{dP_{mc}}{dt} = F_P^{mc} - F_A^{mc} - F_M^{mc} - F_R^{mc} \quad (12)$$

$$\frac{dC_{mantle}}{dt} = F_R^{cc} + F_R^{mc} - F_D \quad (13)$$

$$\frac{dM_{Ca}}{dt} = F_W^{cc} + F_W^{cs} + F_V - F_P^{cc} \quad (14)$$

$$\frac{dM_{Mg}}{dt} = F_W^{mc} + F_W^{ms} - F_V - F_P^{mc} \quad (15)$$

where cc = calcium carbonate, mc = magnesium carbonate, cs = calcium silicate and ms = magnesium silicate. L represents the continental reservoir, P represents the seafloor reservoir, M represents the oceanic reservoir, and C_{mantle} represents the amount of carbon in the mantle, F_W, F_P, F_A, F_R, F_M and F_D are the fluxes of weathering, carbonate precipitation, carbonate accretion, carbonate regassing (subduction), carbonate metamorphism followed by CO_2 degassing, and CO_2 degassing at the mid-ocean ridge, respectively. F_V is the flux of calcium ions produced by volcanic–seawater (hydrothermal) reaction [23,24]:

$$Mg^{2+} + CaSiO_3 \rightarrow MgSiO_3 + Ca^{2+} \quad (16)$$

The fluxes are expressed as follows:

$$F_W = K_W^f(P_{CO_2}, T_S) \cdot L \quad (17)$$

$$K_W^f = K_W \cdot \left(\frac{P_{CO_2}}{P_{CO_2}^*}\right)^{0.3} \cdot \exp\left(\frac{T_S - 285}{13.7}\right) \cdot a \cdot b \quad (18)$$

$$F_A = A \cdot t_r^{-1} \cdot P \tag{19}$$

$$F_R = (1-A) \cdot R \cdot t_r^{-1} \cdot P \tag{20}$$

$$F_M = (1-A) \cdot (1-R) \cdot t_r^{-1} \cdot P \tag{21}$$

$$F_V = K_V \cdot f_q \cdot M_{Mg} \tag{22}$$

where K_W is a constant, P_{CO_2} is the partial pressure of CO_2, T_s is the surface temperature, the superscript $*$ represents the present value, a and b are correction factors [16], t_r is the average residence time of the oceanic plate, A and R are free parameters named accretion ratio and regassing ratio, respectively, and f_q is the heat flow at a given time normalized by the present heat flow. The accretion ratio is defined as the fraction of seafloor carbonates accreted to the continent to the total seafloor carbonates. The regassing ratio is defined as the fraction of seafloor carbonates regassed into the mantle to the total subducting carbonates. F_D will be defined in a later section. F_P is determined so as to sustain a chemical equilibrium among the carbon-related species in the atmosphere, the oceans, and the seafloor, as follows:

$$CO_2(g) + H_2O \leftrightarrow H_2CO_3 \tag{23}$$

$$H_2CO_3 \leftrightarrow HCO_3^- + H^+ \tag{24}$$

$$HCO_3^- \leftrightarrow CO_3^{2-} + H^+ \tag{25}$$

$$Ca^{2+} + CO_3^{2-} \leftrightarrow CaCO_3 \tag{26}$$

$$Mg^{2+} + CO_3^{2-} \leftrightarrow MgCO_3 \tag{27}$$

Further details are described in our previous paper [16].

As the external conditions, which strongly affect the terrestrial environment but are not constrained by the global carbon cycle system, we consider the solar luminosity L, the continental surface area S_C, and the seafloor spreading rate SR. The solar luminosity is considered to have increased by 30% during the history of the Earth [12–15]. We adopt the evolution model proposed by Gough [14]: .

$$L(t) = \left[1 + \frac{2}{5}\left(1 - \frac{t}{t^*}\right)\right]^{-1} \cdot L^* \tag{28}$$

where L is the solar luminosity, t is the time, and $*$ represents the present value. We use the continental growth model proposed by Reymer and Schubert [25]. The seafloor spreading rate is determined from the heat flow calculated from the thermal evolution of the mantle, as will be described later. We use the numerical results of Kasting and Ackerman [26] to calculate the surface temperature T_s as a function of partial pressure of CO_2 in the atmosphere and the luminosity of the sun.

It is difficult to estimate the ocean pH during the history of the Earth because we do not know the alkalinity or the composition of seawater in the past. Therefore, in our previous paper [16], the pH of the seawater was given as a free parameter. However, Walker [27] estimated possible limits on the composition and pH of the Archean seawater from the geochemical record. According to Walker [27], the composition and pH of seawater were given as a function of the partial pressure of CO_2 in the atmosphere. We use his result for estimating the ocean pH as a function of partial pressure of CO_2 in the atmosphere. The ocean pH is iteratively determined by Walker's estimates so that the atmospheric partial pressure of CO_2 and pH of seawater may maintain the chemical equilibrium among the carbon-related species expressed as equations (23)–(27), and may also conserve the carbon mass within the atmosphere, ocean and seafloor reservoirs.

TABLE 1

Values of the constants used in this study

Constant	Value	Remarks
g	$9.8\ m/s^2$	acceleration due to gravity
α	$3\times10^{-5}\ K^{-1}$	thermal expansivity
k	$4.2\ W/m\ K$	thermal conductivity
κ	$10^{-6}\ m^2/s$	thermal diffusivity
ρC_p	$4.2\times10^{6}\ J/m^3K$	volumetric specific heat
λ	$3.4\times10^{-10}\ yr^{-1}$	average decay constant
Ra_{cr}	1100	critical Rayleigh number
β	0.3	Nusselt–Rayleigh exponent
R_m	6271 km	outer mantle radius
R_c	3471 km	inner mantle radius
α_1	$6.4\times10^{4}\ K$	constant in eq. (42)
α_2	$-6.1\times10^{6}\ K$	constant in eq. (42)
$C_{H_2O}^{bas}$	0.03	water content in basalt layer
ρ_c	$2.95\times10^{3}\ kg/m^3$	density of oceanic crust
d_{hc}	$5\times10^{3}\ m$	average thickness of hydrated crust

3. Thermal evolution model

To estimate the degassing and regassing rates of CO_2, which are probably dependent on the seafloor spreading rate or heat flow from the mantle, we need to calculate the thermal evolution of the mantle. We use the parameterized convection model to calculate the whole mantle convection.

The parameterized convection model was developed by many authors [e.g., 20,28–31]. In this model, the temporal variations of average mantle temperature T_m and heat flow q from the mantle, which is parameterized in terms of the Rayleigh number Ra, are calculated. The equation of conservation of energy is given by:

$$\rho C_p\left(R_m^3 - R_c^3\right)\frac{dT_m}{dt} = -3R_m^2 q + \left(R_m^3 - R_c^3\right)Q \tag{29}$$

where ρ is the density, C_p is the specific heat at constant pressure, and R_m and R_c are the outer and inner radii of the mantle, respectively. Q is the energy production rate by decay of radiogenic heat sources in the mantle:

$$Q = Q_0 \exp(-\lambda t) \tag{30}$$

where Q_0 and λ are constants, and t is the time. Mantle heat flow q is parameterized in terms of the Rayleigh number Ra as follows:

$$q = \frac{k(T_m - T_s)}{R_m - R_c}\left(\frac{Ra}{Ra_{cr}}\right)^{\beta} \tag{31}$$

$$Ra = \frac{g\alpha(T_m - T_s)(R_m - R_c)^3}{\kappa\nu} \tag{32}$$

where k is the thermal conductivity, Ra_{cr} is the critical Rayleigh number, β is a constant empirically determined, g is the acceleration due to gravity, α is the coefficient of thermal expansion, κ is the thermal diffusivity, and ν is the viscosity.

It is known that the kinematic viscosity of the mantle depends on the temperature and volatile content, regarding the latter the water content of the mantle especially [32]. McGovern and Schubert [20] have expressed the parameterization of activation temperature T_A for solid-state creep as a function of water weight fraction x as follows:

$$\nu = \nu_m \exp(T_A/T) \tag{33}$$

$$T_A = \alpha_1 + \alpha_2 \cdot x \tag{34}$$

where ν_m, α_1 and α_2 are constants [20]. Hence, to estimate the viscosity of the mantle we need to know the temporal variation of the water content of the mantle.

According to the results of McGovern and Schubert [20], changes in water content are compensated by changes in average mantle temperature, so that the mantle evolves with the viscosity and convective vigor required to transfer its internally generated heat. Thus, compared to a mantle with volatile-independent rheology the mantle is hotter as a consequence of degassing and colder as a consequence of regassing [20,21]. As will be described in the next section, the degassing rate of volatile components depends not only on the seafloor spreading rate but also on the melt generation depth in the mantle, which is related to the average mantle temperature. Hence it is suggested that the global carbon cycle might be coupled with water exchange between the surface and the mantle. Therefore we also consider the global water cycle in addition to the global carbon cycle. Mass balance equations for water reservoirs are as follows:

$$\frac{dW_{surface}}{dt} = F_D^{H_2O} - F_R^{H_2O} \tag{35}$$

$$\frac{dW_{mantle}}{dt} = F_R^{H_2O} - F_D^{H_2O} \tag{36}$$

where $W_{surface}$ and W_{mantle} are the amount of water in the surface and mantle reservoirs, respectively, $F_D^{H_2O}$ is the degassing rate of water, and $F_R^{H_2O}$ is the regassing rate of water.

We use an expression of water regassing rate similar to that of McGovern and Schubert [20], as follows:

$$F_R^{H_2O} = R_{H_2O} \cdot \left[C_{H_2O}^{bas} \cdot (\rho_c \cdot SR \cdot d_{hc})\right] \tag{37}$$

where R_{H_2O} is the regassing ratio of water, $C_{H_2O}^{bas}$ is the average mass fraction of water in the basal layer, ρ_c is the density of oceanic crust, and d_{hc} is the average thickness of the hydrated oceanic crust. The regassing ratio of water is defined as the fraction of water regassed into the mantle

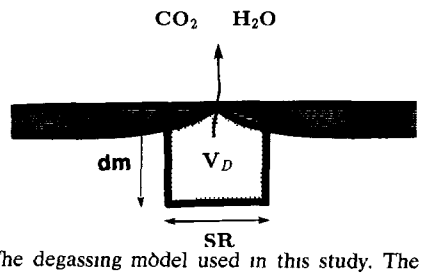

Fig. 2. The degassing model used in this study. The mantle degassing volume is defined by the volume from which volatile components are degassed to the surface when the new oceanic plates are formed This volume is determined by the seafloor spreading rate SR and the melt generation depth d_m in the mantle.

compared to the total subducting water in the hydrated oceanic crust. The regassing rate of carbon was defined in equation (20).

4. Degassing model

Volatile elements in the mantle degas through plate formation at the mid-ocean ridge. When new ocean plates are formed, volatile elements in a certain volume of the mantle degas (Fig. 2). This volume is probably dependent on the seafloor spreading rate SR and the melt generation depth d_m in the mantle. We define the degassing rate of CO_2 from the mantle as follows:

$$F_D^{CO_2} = K_D^{CO_2} \cdot C_{mantle} \tag{38}$$

$$K_D^{CO_2} = f_{CO_2} \cdot V_D / V_{mantle} = f_{CO_2} \cdot SR \cdot d_m / V_{mantle} \tag{39}$$

where $K_D^{CO_2}$ is the coefficient of degassing rate, C_{mantle} is the amount of carbon in the mantle, V_D is the volume of the mantle from which degassing occurs in unit time, and V_{mantle} is the volume of the mantle. f_{CO_2} is the degassing fraction, defined as the fraction of CO_2 that degasses to the surface compared to the total amount of CO_2 that is originally included in the mantle degassing volume V_D.

When partial melting of mantle material occurs, volatile elements partition into the melt according to their partition coefficients, and then these volatile elements finally degas to the surface when magma erupts and solidifies as oceanic crust at the surface. In addition to this, bubbles are formed when upward moving magma becomes supersaturated with one of its major volatile elements due to a decrease in solubility as the pressure decreases [e.g., 33,34]. Bubbles grow in size because of the diffusional flux of dissolved gases and decompression. Volatile elements in these bubbles would also degas to the surface. The content of the bubbles is dominated by CO_2, in general because of its abundance and relatively low solubility [e.g., 34]. The volatile element with greater solubility in the silicate melt would mainly partition to the liquid phase (magma), whereas the volatile element with lower solubility to the silicate melt would partition into the gas (bubble) phase.

We consider a simple case of batch melting as the first approximation. Let us express the mass of solid and liquid phases of mantle materials (W^S and W^L, respectively) and the mass of the volatile elements in the solid, liquid, and gas phases (w^S, w^L, and w^G, respectively). The volatile elements in the gas and liquid phases are assumed to degas to the surface. Then the degassing fraction defined by the mass ratio of element partitioning into the liquid and gas phases to the total mass included originally in the degassing volume is given by [35]:

$$f_i = \frac{1}{1 + \dfrac{(F^{-1} - 1) K_i^{S/L}}{1 + (w^G/w^L)_i}} \tag{40}$$

where the melt fraction F is defined by $F \equiv W^L/(W^S + W^L)$ and $K^{S/L}$ is the partition coefficient. The factor w^G/w^L represents the solubility of volatile elements into the silicate melt. When the bubble consists of mixed gas, the factor w^G/w^L is given by [35]:

$$\left(\frac{w^G}{w^L}\right)_i = \frac{\phi m_i}{\rho_c C_i^L V_{M,i}^T} \frac{n_i}{n} = \frac{\phi m_i}{\rho_c C_i^L V_{M,i}^P} \tag{41}$$

where $\phi = V^G/V^L$ is the vesicularity of MORB, m is the molecular weight, and ρ_c is the density of oceanic crust. n and n_i are the total molar number and the molar number of the volatile component i, respectively, and thus n_i/n represents the molar fraction of gas component i in the vesicles. $V_{M,i}^T$ and $V_{M,i}^P$ are the molar volumes of component i at the total pressure of bubbles

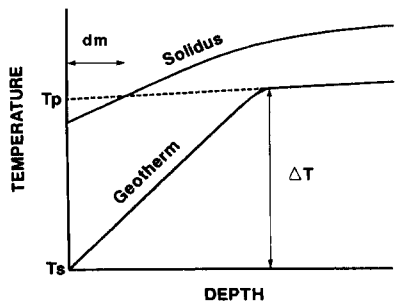

Fig. 3. Schematic diagram of the geotherm and solidus in the mantle. ΔT represents the temperature difference across the thermal boundary layer. The melt generation depth d_m below the mid-ocean ridge is defined by the depth where ascending mantle material intersects the basalt eutectic, and extensive melting and melt segregation occur. We assume that mantle volatile components are released from this depth with the melt segregation.

($P_B \sim 0.25$ kbar) and at its partial pressure ($P_{B,i} = (n_i/n) \times P_B$), respectively.

We obtain $V^T_{M,CO_2} = 517 \times 10^{-6}$ m^3/mol using the Redlich–Kwong equation of state. If we choose $C^L_{CO_2} \sim 100 \times 10^{-6}$ g/g, $n_{CO_2}/n \sim 0.8$, $m_{CO_2} = 44 \times 10^{-3}$ kg/mol, $\rho_c \sim 3 \times 10^3$ kg/cm^3, $\phi \sim 1.5\%$, and $K^{S/L} = 2.36$, f_{CO_2} is estimated to be 0.32 [35].

The degassing rate of water is also defined as follows:

$$F_D^{H_2O} = K_D^{H_2O} \cdot W_{mantle} = f_{H_2O} \cdot SR \cdot d_m / V_{mantle} \tag{42}$$

where f_{H_2O} is estimated to be 0.194 [35].

The seafloor spreading rate as a function of mantle heat flow is given by a cooling model of the oceanic plate, such as cooling of a semi-infinite half-space. The relation between the heat flow q and the average residence time of the oceanic plate t_r is expressed as follows [36]:

$$q = \frac{2k\Delta T}{\sqrt{\pi \kappa t_r}} \tag{43}$$

where ΔT is the temperature difference across the thermal boundary layer at the surface. We approximate $\Delta T \sim T_p - T_s$, where T_p is the potential temperature of the mantle and T_s is the surface temperature (Fig. 3). The average residence time of the oceanic plate t_r is given by

$$t_r = \frac{S_O}{SR} = \frac{S_E - S_C}{SR} \tag{44}$$

where S_O is the area of the ocean floor and S_E is the surface area of the Earth. Using eqs. (43) and (44), SR is given by:

$$SR = \frac{\pi \kappa (S_E - S_C)}{(2k\Delta T)^2} \cdot q^2 \tag{45}$$

The melt generation depth below the mid-ocean ridge is about 40 km at present [37]. It is defined by the depth where the ascending mantle material intersects the basalt eutectic, and thus extensive melting and melt segregation occur at this depth (Fig. 3). We assume that mantle volatile components are released with the melt segregation effectively at this depth. To estimate the melt generation depth at a given time, we need to know the solidus temperature of the mantle material and the temporal variation of potential temperature of the mantle.

McKenzie and Bickle [37] have compiled experimental results on the solidus temperature of mantle material, and parameterized them to obtain an analytical expression:

$$P = (T_{sol} - 1100)/136 + 4.968 \times 10^{-4} \times \exp\left[1.2 \times 10^{-2}(T_{sol} - 1100)\right] \tag{46}$$

where P is the pressure (GPa) and T_{sol} is the solidus temperature (°C).

The average mantle temperature T_m obtained by solving the equation of conservation of energy is expressed by:

$$T_m = \frac{\int \rho C_p T(r)\, dV}{\int \rho C_p\, dV} \tag{47}$$

where $T(r)$ is the actual mantle temperature at position r and the integrals extend over the mantle volume [30].

The potential temperature, T_p, on the other hand, is defined as the temperature of a fluid mass compressed or expanded adiabatically to some constant reference pressure (the surface pressure in this case). At present, this potential temperature of the mantle below the mid-ocean ridge is estimated to be 1280°C [37]. The heat transport by mantle convection may result in the adiabatic temperature gradient in the mantle, expressed as $(\partial T/\partial r)_S = -g\alpha T/C_p$. Assuming an adiabatic temperature gradient in the convecting

mantle, we can obtain the potential temperature by integrating the above equation from a certain depth ($r' = r$) to the surface ($r = R_s$):

$$T_p = T(r) \exp\left(-\int \frac{g\alpha}{C_p} \, dr' \right) \tag{48}$$

therefore

$$T(r) = T_p \exp\left(\int \frac{g\alpha}{C_p} \, dr' \right) \tag{49}$$

Using eq. (49), T_m is given by:

$$T_m = \frac{\int \rho C_p \exp\left(\int \frac{g\alpha}{C_p} \, dr' \right) dV}{\int \rho C_p \, dV} \cdot T_p \tag{50}$$

therefore

$$T_p = \frac{\int \rho C_p r'^2 \, dr'}{\int \rho C_p \exp\left(\int \frac{g\alpha}{C_p} \, dr' \right) r'^2 \, dr'} \cdot T_m = \gamma \cdot T_m \tag{51}$$

where

$$\gamma = \frac{\int \rho C_p r'^2 \, dr'}{\int \rho C_p \exp\left(\int \frac{g\alpha}{C_p} \, dr' \right) r'^2 \, dr'} \tag{52}$$

Thus we can estimate the potential temperature from the average temperature of the mantle. We estimated the value of γ to be about 0.6–0.8 by integrating eq. (52) numerically. The uncertainty in the above estimate is mainly due to the uncertainty in the structure of thermal expansivity in the mantle. We use the average value ($\gamma = 0.7$) in this study. The melt generation depth can be obtained by solving eqs. (46) and (49) numerically under the condition of hydrostatic equilibrium. It is noted that the coefficient of degassing rate varies with time when the seafloor spreading rate and the melt generation depth change.

5. Total amount of carbon

The total amounts of carbon and water are assumed to be given by summation of the amount of these components in the surface and mantle reservoirs, i.e. $C_{total} = C_{surface} + C_{mantle}$ and $W_{total} = W_{surface} + W_{mantle}$, where C and W represent the amount of carbon and water, respectively.

The present amount of carbon at the surface of the Earth has been estimated by many geochemists [e.g., 38–40]. In this study, we assume about 1×10^{22} mol ($\sim 1.2 \times 10^{20}$ (C) kg) as the present amount of surface carbon, according to the estimate of Ronov and Yaroshevsky [40].

The amount of carbon in the mantle is rather difficult to estimate. However, if the CO_2 degassing rate is given by the mantle degassing volume multiplied by the CO_2 concentration in the mantle, the amount of mantle CO_2 can be estimated from the observational data. The present seafloor spreading rate is 2.84×10^{12} m^2/Ma [36] and the present melt generation depth is 40 km [37]. Thus the mantle degassing volume from which degassing occurs at the present time is $V_D^* = SR^* \times d_m^* = 11.4 \times 10^{16}$ m^3/Ma. Recent estimates of the CO_2 degassing rate at the mid-ocean ridge are about 2.2×10^{18} mol/Ma [41]. The abundance of carbon in the mantle is thus obtained from eqs. (38) and (39) as $C^*_{mantle}/V_{mantle} = F_D^*/V_D^* f_{CO_2} = 156$ ppm [35]. This is considered to correspond to the abundance of carbon in the upper mantle. If we assume a homogeneous mantle, we obtain an amount of mantle carbon of about 5.2×10^{22} mol. This is about five times the present amount of surface carbon. The total amount of carbon retained in the surface and mantle reservoirs is thus estimated to be about 6.2×10^{22} mol or 7.4×10^{20} (C) kg at present. This estimation derived from assuming a homogeneous mantle would give a lower estimate for the amount of mantle carbon because the upper mantle might be a depleted and degassed mantle. It is, however, noted that an estimate such as the one mentioned above is required for self-consistency of the model.

Although this estimate gives a rather small value of $C/^{36}Ar$ in comparison with that of various meteorites [42], it does satisfy the upper limit of the amount of CO_2 in the proto-atmosphere, which is constrained by the condition necessary for the formation of the ocean [43]. We assume mass conservation of carbon within the surface reservoirs and the mantle throughout the entire history of the Earth.

The amount of surface water is 7.8×10^{22} mol at present. We can estimate the abundance of mantle water by using a method similar to that used for carbon. The degassing rate of H_2O at the mid-ocean ridge was estimated to be $\sim 1.1 \times 10^{17}$ kg/Ma by Ito et al. [44]. Therefore, the amount of mantle water is estimated to be 0.1 ppm or 2.4×10^{23} mol [35].

6. Initial conditions and other model parameters

During the accretion of the Earth, volatile components in planetesimals should have been degassed by impacts, because the peak pressure produced by impacts is high enough to cause impact degassing [3]. The amount of impact-induced steam atmosphere might be determined by the dissolution equilibrium between the atmosphere and the magma ocean [1–4], although detailed chemical forms and the volatile partitioning between the mantle and the core may depend on the process of core formation and the oxygen fugacity in the proto-mantle. According to Matsui and Abe [5,6], the initial amount of water at the surface is $W^0_{\text{surface}} \sim W^*_{\text{surface}}$, where the superscript 0 represents the initial value and * represents the present value. The degree of melting of the magma ocean is estimated to be about 10% for the most probable case [2]. From the distribution coefficient of CO_2 at this degree of melting, about 80% of CO_2 occurs in the atmosphere [42]. If the total amount of carbon at the end of accretion remains in the surface layers, the initial amount of carbon at the surface is $C^0_{\text{surface}} = 0.8 \cdot C_{\text{total}}$. We call the model with these initial conditions the standard case, and name it "case 1".

For comparison, we consider two other cases with different initial amounts of volatile components at the surface. One is the case for no initial atmosphere (case 2: $C^0_{\text{surface}} = 0$, $W^0_{\text{surface}} = 0$) and the other is the completely degassed case (case 3: $C^0_{\text{surface}} = C_{\text{total}}$, $W^0_{\text{surface}} = W_{\text{total}}$).

The initial average temperature of the mantle would have a significant influence on the early degassing history, but it cannot be determined from the thermal evolution model. This is because the mantle cannot retain any information on its initial condition at present [e.g., 29,31]. Nevertheless we consider that the hot origin of the Earth is more reasonable than the cold one because the proto-Earth would retain a large amount of gravitational energy liberated during accretion and core formation [e.g., 1–4]. The initial temperature profile of the proto-mantle might be approximated by the solidus temperature.

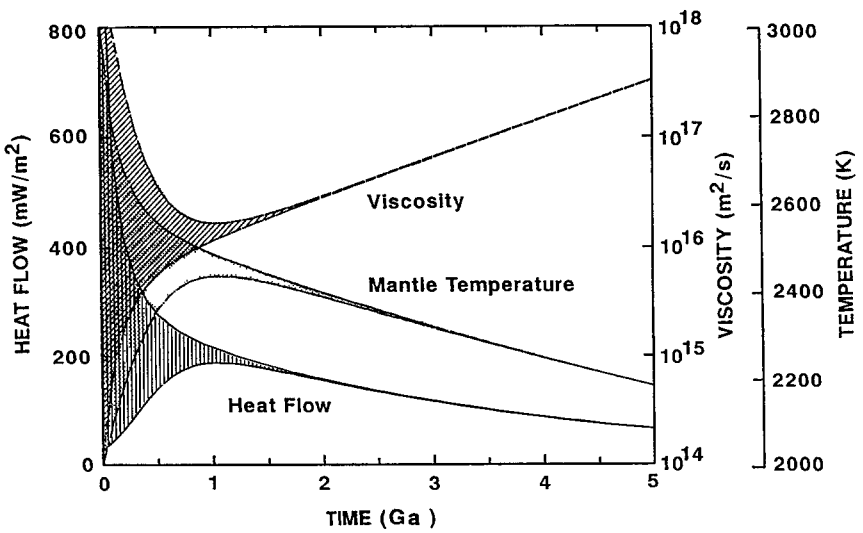

Fig. 4. Temporal variations of mantle viscosity, average mantle temperature and mantle heat flow for case 1. The initial mantle temperature is assumed to be 2000–3000 K (the hatched area). These results are qualitatively similar to those of previous studies [20,28–31].

However, we assumed simply the initial average mantle temperature to be 2000–3000 K in this study.

Other parameters are determined as follows: The value of the coefficient of radiogenic heat production rate Q_0 is iteratively adjusted so that the mantle heat flow at $t = 4.6 \times 10^9$ yrs may be equal to the present value ($q^* = 70$ mW/m^2 [36]). The accretion ratio A affects both the amount of surface carbon and its distribution among surface reservoirs, whereas the regassing ratio R does not have a large affect on the distribution and amount of surface carbon [16]. We assume the accretion ratio to be around 0.7, as discussed in our previous paper [16]. The regassing ratio of water R_{H_2O} is iteratively adjusted so that the amount of surface water at $t = 4.6 \times 10^9$ yrs may be equal to the present value ($= 1.4 \times 10^{21}$ kg). The other parameter values are summarized in Table 1.

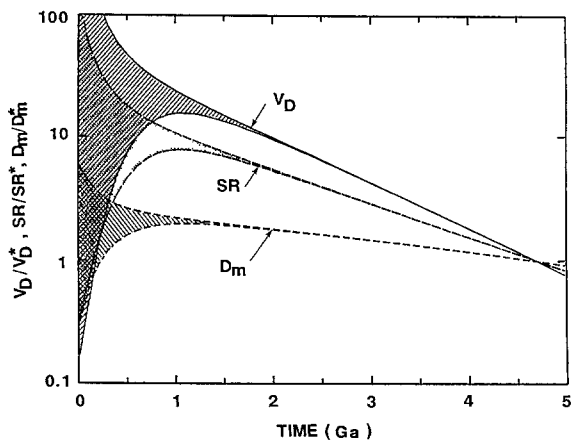

Fig. 5 Temporal variations of seafloor spreading rate, melt generation depth and mantle degassing volume for case 1. The initial mantle temperature is assumed to be 2000–3000 K (the hatched area). Note that the mantle degassing volume was much greater in the Hadean and Archean periods than at present This implies more effective degassing in the Hadean and Archean.

7. Numerical results

Figure 4 shows the numerical results for case 1. The temporal variation of mantle viscosity, average mantle temperature, and mantle heat flow are shown for the initial average temperature 2000–3000 K. These physical quantities begin to converge rapidly into a very narrow range during the early stage of Earth history. This means, as mentioned previously, that the present mantle has not retained any information on the initial mantle temperature. The average mantle temperature and mantle heat flow decreased monotonically thereafter, but the mantle viscosity increased with a decrease in mantle temperature. In our model the mantle viscosity is assumed to depend on the mantle temperature and water content. The mantle temperature is therefore determined so that convective vigor for internal heat transfer may be sustained, which compensates the change in viscosity due to change in water content [see 20].

Figure 5 shows the temporal variation of seafloor spreading rate, melt generation depth, and mantle degassing volume (from which the degassing is assumed to occur) for case 1. As shown in this figure, the above quantities have decreased monotonically to the present quantities. The seafloor spreading rate in the Archean is estimated to have been 4–16 times greater than today's rate. The melt generation depth at that time was about 70–100 km, which is about 2–2.5 times greater than the present time in this model. As a consequence, the mantle degassing volume in the Archean was about 8–40 times greater than the present volume. Therefore, according to this model, it is strongly suggested that the effective degassing would have occurred in the Hadean and Archean periods.

Figure 6 shows the temporal variations in the rate of CO_2 degassing and regassing and the amount of surface carbon for case 1. As expected, both degassing and regassing rates in the Hadean and Archean were much greater than those of today. Regassing rather than degassing was much more effective in the early stage because 80% of the total amount of carbon had initially been at the surface in this case. As the degassing and regassing rates became balanced, the amount of surface carbon approached a stationary level. This feature is also seen in the results for the other cases.

Figure 7 shows the temporal variation of the amount of surface carbon for three cases. In each case, the amount of surface carbon approaches the present level. This may imply that the present state of the surface carbon is in a steady state and the present amount is not influenced by the ini-

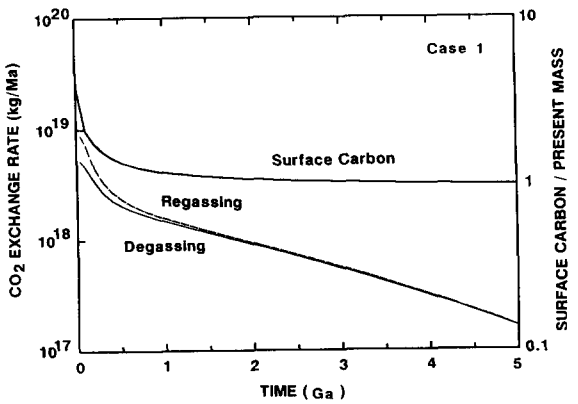

Fig. 6. Temporal variations of CO_2 degassing and regassing rates and the amount of surface carbon for case 1 (the initial mantle temperature is 3000 K) Both degassing and regassing rates in the Hadean and Archean are much greater than those of today. When the degassing and regassing rates become equally balanced the amount of surface carbon approaches a stationary level.

tial amount. The response time of surface carbon against the perturbation under the present condition will be estimated in the next section. According to the CO_2 degassing and regassing rates shown in Fig. 6, the surface carbon could be suggested to have been circulated several times over the entire history of the Earth. This issue too will be discussed in the next section.

Figure 8 shows the temporal variations in the amount of surface water for three cases. The amount of surface water increased at beginning

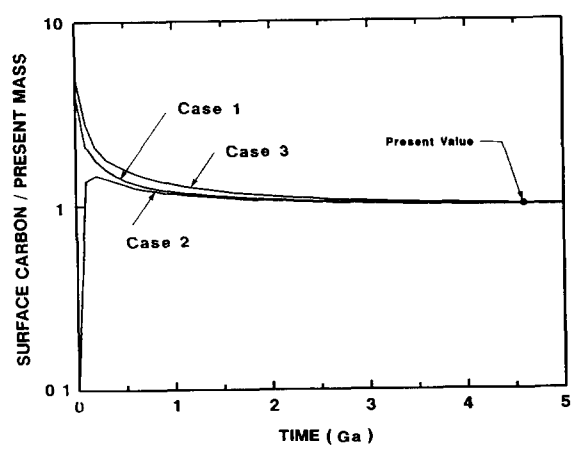

Fig. 7. Temporal variations in the amount of surface carbon for three cases (the initial mantle temperature is 3000 K). Note that in every case the amount of surface carbon reaches a stationary level.

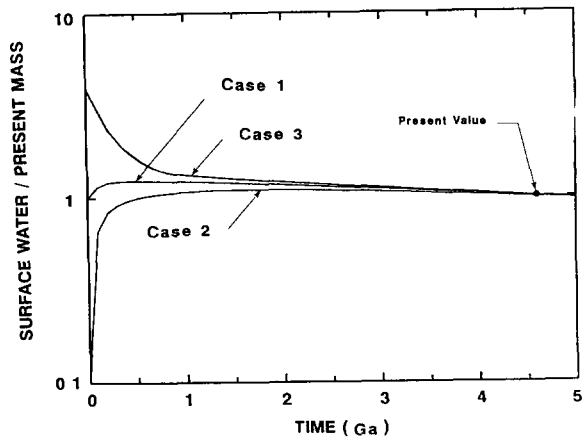

Fig. 8 Temporal variations in the amount of surface water for three cases (the initial mantle temperature is 3000 K). The amount of surface water increases at the early stage of evolution and then slightly decreases to the present value.

for the cases 1 and 2, and then decreased slightly to the present value. The water regassing rate is influenced by the seafloor spreading rate, but not by the amount of surface water. The water degassing rate, on the other hand, depends not only on the seafloor spreading rate but also on the melt generation depth and the amount of mantle water. Hence the change in water degassing rate is much greater than that in the water regassing rate. In this respect, the temporal variation of the amount of surface water is controlled mainly by the temporal variation of the rate of degassing of water from the mantle.

Figure 9 shows the temporal variations of the content of the surface carbon reservoirs and the surface temperature for case 1. The amount of CO_2 in the proto-atmosphere has decreased with time, which results in stabilization of the surface temperature against an increase in the solar luminosity. The reason is as follows: once the continents were formed, they supplied a large quantity of cations to the oceans by weathering, resulting in consumption of atmospheric CO_2 and thus an increase in precipitation of carbon as carbonates on the seafloor. The partial pressure of atmospheric CO_2 in the Archean was probably about 100–1000 times the present value, thus being required for maintaining the surface temperature above the freezing point of water at that time. Because of a negative feedback mechanism for the surface temperature, which is a crucial fea-

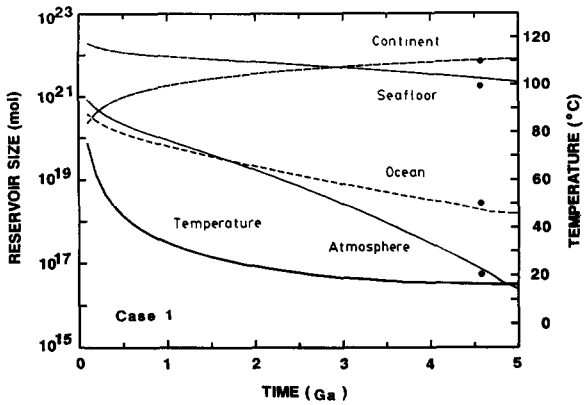

Fig. 9. Temporal variations in the surface temperature and the content of the surface carbon reservoirs. The dots represent the present values. The amount of CO_2 in the proto-atmosphere decreased with time, which results in stabilization of the surface temperature against an increase in the solar luminosity

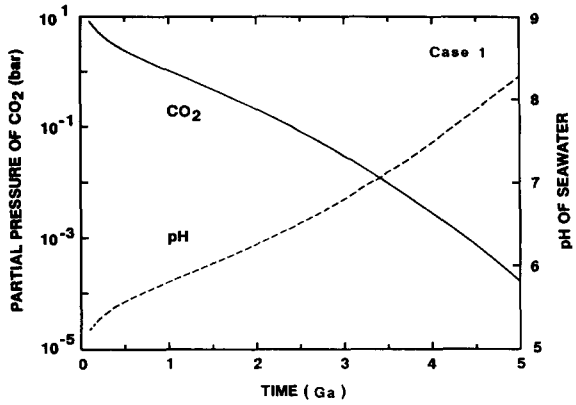

Fig. 10 Temporal variations in pH of seawater and CO_2 in the atmosphere. pH of seawater increases with a decrease in partial pressure of CO_2, from about 5 to the present value 8.

ture of the carbon cycle system [e.g., 16,17], the temperature would have been maintained around the present value after the continents grew to almost their present size (> 1.0 Ga). This suggests that even when we take into account the degassing rate of CO_2 coupled with the thermal history of the mantle, the terrestrial environment was stabilized by a negative feedback mechanism for the surface temperature by the time large continents were formed [see 16]. However, it is noted that the effective weathering rate might be high during the first 1.0 Ga of Earth's history. This is because impacts during heavy bombardment would stir up much fine ejecta, which might be weathered more effectively. As a consequence, the partial pressure of CO_2 and the surface temperature might have been lower at that time.

The distribution of carbon among the atmosphere and the ocean is determined by the pH of the ocean, which we estimated iteratively in this study. The temporal variation of the pH of the seawater and partial pressure of CO_2 in the atmosphere are shown in Fig. 10. A decrease in the partial pressure of CO_2 in the atmosphere results in maintaining the surface temperature around its present value. Seeing as we use the relationship between the ocean pH and the partial pressure of atmospheric CO_2 proposed by Walker [27], the ocean pH increases with the decrease in partial pressure of CO_2 from about 5 to the present value 8. The corresponding temporal variations of the amount of bicarbonate, carbonate, calcium and magnesium ions in the ocean are shown in Fig. 11. The amount of bicarbonate ions decreases with a decrease in atmospheric CO_2. The amount of carbonate ions, however, increases with time. This is because the amount of carbonate ions is strongly dependent on the pH of the seawater. The ratio of bicarbonate ion to carbonate ion depends on the pH value η, such that $M_{HCO_3^-}/M_{CO_3^{2-}} \propto a_{H^+} \propto 10^{-\eta}$, where a_{H^+} is the activity of the hydrogen ion (see eq. 25). Hence the ratio $M_{HCO_3^-}/M_{CO_3^{2-}}$ decreases with the increase in the pH of the seawater, which results in an increase in the amount of carbonate ion with

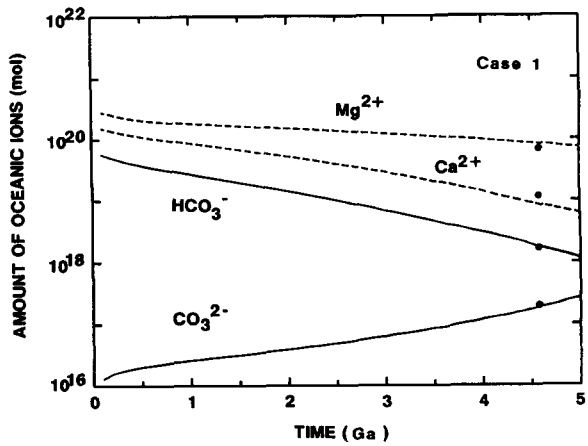

Fig. 11. Temporal variations of bicarbonate, carbonate, calcium and magnesium ions in the ocean. The dots represent the present values. See text for further details.

time. The calcium ion is always in chemical equilibrium with calcium carbonate (calcite), and thus the calcium ion decreases with time. The magnesium ion, however, is determined from a balance between the supply of the magnesium ion by weathering of the continents and consumption by hydrothermal reaction at the mid-ocean ridge over the entire history of the Earth. The magnesium ion is not in chemical equilibrium with magnesium carbonate (magnesite). This differs from the result of the previous study [16], in which pH was assumed to be constant (present value). In such cases, the magnesium ion is in chemical equilibrium with magnesite until the early Archean [16].

8. Discussion

The temporal variation of seafloor spreading rate exerts a significant influence on volatile exchange between the surface reservoirs and the mantle. Seafloor spreading followed by subduction results in circulation of surface carbon into the mantle. The amount (or the frequency) of carbon circulation depends on variation in the seafloor spreading rate over the history of the Earth. The circulation of carbon between the surface reservoirs and the mantle is related to carbon isotope variation. Carbon has two stable isotopes, ^{12}C and ^{13}C. The difference in $^{13}C/^{12}C$ from the standard sample is usually expressed as $\delta^{13}C$, and is defined as follows:

$$\delta^{13}C = \left[\frac{(^{13}C/^{12}C)_{sample}}{(^{13}C/^{12}C)_{standard}} - 1 \right] \times 1{,}000‰ \quad (53)$$

where the subscript "standard" conventionally refers to the carbonate skeleton of the fossil Peedee Belemnite, whose $^{12}C/^{13}C$ is 88.99. The $\delta^{13}C$ values of the carbonate and the organic carbon are known to have been almost constant, about 0‰ and −25‰ respectively, since at least the oldest record, which dates back to 3.5 billion years (and probably 3.8 billion years) ago [45–47]. The $\delta^{13}C$ in the mantle has also been estimated to be constant (about −5‰), from samples such as old diamonds, carbonatites, carbonate from kimberlites and present-day mid-ocean ridge basalt [45–48]. The constancy of these isotope data suggests that the mantle carbon ($\delta^{13}C = -5‰$) was degassed to the surface, where carbon has been depositing as carbonate ($\delta^{13}C = 0‰$) and organic carbon ($\delta^{13}C = -25‰$) at a constant ratio of 4:1 since at least 3.5 billion years ago [45–47].

This causes the problem of the effect of isotope fractionation associated with the subduction of carbonate and organic carbon into the mantle. The degree of metamorphism at a subduction zone differs, in general, between carbonate and organic carbon. This means that the carbon isotope regassed into the mantle would be different from that degassed into the atmosphere. Hence the carbon isotope in the mantle would have varied through carbon exchange between the surface and the mantle during the history of the Earth. However, the present-day mantle inferred from the mid-ocean ridge basalts and hydrothermal fluids still retains the $\delta^{13}C$ value of around −5‰ [e.g., 48].

Although the volatile exchange rates would have been greater during the earliest evolution of the Earth (Fig. 6), the frequency of carbon circulation between the surface reservoirs and the mantle becomes important only after the organic activities, which fractionate the carbon isotopes, become effective. Such activities became effective about 3.5–3.8 billion years ago [46]. We do not know how much the carbon isotope would be fractionated in one cycle, but it may be reasonably assumed that the total volume of degassed mantle since 3.5×10^9 yrs ago is, at least, less than the total volume of the mantle:

$$\int f_{CO_2} \cdot V_D(t)\, dt < V_{mantle} \quad (54)$$

where f_{CO_2} is the degassing fraction of CO_2, V_D is the degassing volume per unit time and V_{mantle} is the volume of the mantle. We therefore define the frequency of carbon circulation through the mantle reservoir N_{mantle} by the following relation and give the above condition as follows:

$$N_{mantle} = \frac{\int f_{CO_2} \cdot V_D(t)\, dt}{V_{mantle}} < 1 \quad (55)$$

The frequencies of carbon circulation between the surface reservoirs and the mantle after 3.5 billion years ago are estimated from our numerical simulation, as shown in Table 2. These values do not depend much on the initial average man-

TABLE 2

Frequencies of carbon circulation after 3.5 billion years ago

Seafloor spreading rate	Initial mantle temperature (K)	$N^*_{surface}$	N^{**}_{mantle}
variable***	3000	22.7	4.55
	2500	8.2	1.65
	2000	4.8	0.95
constant	2500	1.7	0.34
	2000	1.1	0 22

* $N_{surface}$ represents the frequency of carbon circulation through the surface reservoir

** N_{mantle} represents the frequency of carbon circulation through the mantle reservoir

tle temperature because it converged rapidly to a narrow range before 3.5 Ga ago (Fig. 4). From the above discussion, these values may suggest that the model with the seafloor spreading rate constrained by the thermal history calculation results in the circulation of too much volatile for maintaining the carbon isotope ratio in the mantle at a constant level against the isotope fractionation due to the global carbon cycle (i.e., $N_{mantle} > 1$). However, carbon and sulfur isotopic ratios in the sediments seem to be interrelated, so that their behavior leads us to assume that the sediment/ocean is a closed system [e.g., 47]. This implies that carbon exchanges between the surface reservoirs and the mantle might be small.

As a comparison, we consider another model in which a constant seafloor spreading rate (= present value) is assumed throughout the entire history of the Earth. In this case, the mantle heat flow is obtained from the seafloor spreading rate using eqs. (43) and (44). The results for such a model are shown in Table 2. The constant spreading rate model results in a reasonable frequency of carbon circulation (i.e., $N_{mantle} < 1$). This result is consistent with that estimated from the degassing history of ^{40}Ar, which also suggests that the seafloor spreading rate was almost the same as that of today [28,49]. Because carbon is a major component of the degassing gases at the mid-ocean ridge, whereas argon is a minor component, we may suggest that the seafloor spreading rate may not have changed greatly compared to its present value. This corresponds to the numerical results of the parameterized convection model with $\beta = 0$ [31]. It may also support the idea that the seafloor spreading rate is determined not by the convective vigor in the mantle but by the balance of forces such as the slab pull and slab resistance [50]. The frequency of carbon circulation through the surface reservoirs $N_{surface}$ is about 1–2 in this case (Table 2). This is because $N_{surface} \sim 5N_{mantle}$ (i.e., the mantle carbon reservoir is about five times larger than the surface carbon reservoir, as estimated earlier).

Carbon isotope mixing in the mantle after subduction of seafloor sediments would actually be related to mantle dynamics, but this goes beyond the purposes of this study.

We found that the present amount of surface carbon is in steady state and that it could not be influenced by the initial amount of surface carbon. Here we discuss the stability of the present carbon cycle system. For this purpose, we need to estimate the response time against the perturbation for surface carbon under present conditions. The mass balance equation for the present surface carbon in steady state is given by:

$$\frac{dC_{surface}}{dt} = F^*_D - F^*_R = K^*_D \cdot C^*_{mantle} - K^*_R \cdot P^* = 0 \quad (56)$$

where

$$K^*_D = f_{CO_2} \cdot V^*_D / V_{mantle} \sim 4.2 \times 10^{-5} Ma^{-1} \quad (57)$$

$$K^*_R = (1 - A) R / t^*_r \sim 1.1 \times 10^{-3} Ma^{-1} \quad (58)$$

When $C^*_{surface}$ is perturbed to be $C^*_{surface} + \delta C$ by sudden large (or small) degassing (or regassing), eq. (56) becomes:

$$\frac{d(C^*_{surface} + \delta C)}{dt} = K^*_D (C^*_{mantle} - \delta C) - K^*_R (P^* + \delta C) \quad (59)$$

Here we assume that the amount of perturbed carbon δC affects the amount of seafloor carbonate P directly through the continental weathering followed by the carbonate precipitation. Therefore, by subtracting eq. (56) from eq. (59) we obtain the following equation:

$$\frac{d\delta C}{dt} = -(K^*_D + K^*_R) \cdot \delta C \quad (60)$$

This equation can be solved easily, as follows:

$$\delta C = \delta C^0 \cdot e^{-(K^*_D + K^*_R) t} \quad (61)$$

where δC^0 is a constant. Hence the response time τ for the perturbation is:

$$\tau \sim (K_D^* + K_R^*)^{-1} \sim 875 \text{ Ma} \quad (62)$$

This supports the idea that the present carbon cycle might be in steady state. It would take less than 900 million years to achieve the present-day steady state against the perturbation for the surface carbon due to sudden large-scale degassing or small-scale regassing. The present carbon cycle system would not be influenced by the initial amount of surface carbon because of this short characteristic time scale.

9. Summary

The main results of this study can be summarized as follows:

(1) The amount of surface carbon at the present time seems to be in steady state. Hence the present amount of surface carbon may not be influenced by the initial amount of surface carbon.

(2) The response time of the global carbon cycle system against the perturbation for surface carbon under the present condition is estimated to be less than 900 million years.

(3) Continental growth is required for the terrestrial environment to be stabilized against an increase in the solar luminosity.

(4) In the Archean the partial pressure of CO_2 in the atmosphere would have been about 100–1000 times the present level. This is probably one reason why a climate similar to that of the present Earth prevailed under the lower solar constant at that time.

(5) Ocean pH might have been lower in the past, the result of higher partial pressure of CO_2. Calcium ions in the ocean have been in chemical equilibrium with carbonate ions throughout the history of the Earth. Magnesium ions, however, have been out of equilibrium with magnesite. Consumption of magnesium ions by hydrothermal reaction at the mid-ocean ridges and its supply by continental weathering would have been balanced over the history of the Earth.

(6) The seafloor spreading rate might have been almost constant throughout the history of the Earth to explain the frequency of carbon circulation into the mantle; this is suggested from the apparent constancy of the carbon isotope ratio in the mantle since about 3.5 billion years ago.

(7) Carbon at the surface may probably have been circulated between the surface reservoirs and the mantle once or twice since the Archean.

(8) The amount of CO_2 in the present mantle is estimated to be more than 5×10^{22} mol (about five times the present surface value).

Acknowledgements

This research was partially supported by grants-in-aid for Scientific Research (No. 02804023) of the Ministry of Education of Japan. The numerical calculations were performed by M-680H/M-682H at the Computer Center of the University of Tokyo.

References

1 Y Abe and T Matsui, The formation of an impact-induced H_2O atmosphere and its implications for the early thermal history of the Earth, in. Proc. Lunar Planet Sci Conf. 15th, J Geophys Res. 90, C545–C559, 1985.

2 Y Abe and T Matsui, Early evolution of the Earth accretion, atmosphere formation and thermal history, in· Proc Lunar Planet Sci. Conf 17th, J Geophys Res 91, E291–E302, 1986

3 T Matsui and Y Abe, Evolution of an impact-induced atmosphere and magma ocean on the accreting Earth, Nature 319, 303–305, 1986

4 K.J Zahnle, J.F. Kasting and J B Pollack, Evolution of a steam atmosphere during Earth's formation, Icarus 74, 62–97, 1988

5 T Matsui and Y. Abe, Impact-induced atmospheres and oceans on Earth and Venus, Nature 322, 526–528, 1986

6 Y Abe and T. Matsui, Evolution of an impact-generated H_2O–CO_2 atmosphere and formation of a hot proto-ocean on Earth, J Atmos Sci 45, 3081–3101, 1988.

7 J W. Larimer, Composition of the Earth. Chondritic or achondritic?, Geochim. Cosmochim. Acta 35, 769–786, 1971

8 T Owen, R D Cess and V Ramanathan, Early Earth. An enhanced carbon dioxide greenhouse to compensate for reduced solar luminosity, Nature 277, 640–642, 1979

9 W R Kuhn and J F Kasting, Effect of increased CO_2 concentrations on surface temperature of the early Earth, Nature 301, 53–55, 1983

10 J C.G Walker, Climatic factors on the Archean Earth, Palaeogeogr , Palaeoclimatol Palaeoecol 40, 1–11, 1982

11 J F Kasting, Theoretical constraints on oxygen and carbon dioxide concentrations in the Precambrian atmosphere, Precambrian Res 34, 205–229, 1987

12 C. Sagan and G. Mullen, Earth and Mars: Evolution of atmospheres and surface temperatures, Science 177, 52–56, 1972
13 M.J. Newman and R.T Road, Implications of solar evolution for the Earth's early atmosphere, Nature 198, 1035–1037, 1972.
14 D.O. Gough, Solar interior structure and luminosity variations, Sol. Phys. 74, 21–34, 1981.
15 R.L. Gilliland, Solar evolution, Palaeogeogr, Palaeoclimatol. Palaeoecol. (Global Planet. Change Sect.) 75, 35–55, 1989.
16 E. Tajika and T. Matsui, The evolution of the terrestrial environment, in: Origin of the Earth, H.E. Newsom and J.H. Jones, eds., pp. 347–370, Oxford Univ. Press, 1990.
17 J.C G. Walker, P.B. Hays and J F Kasting, A negative feedback mechanism for the long-term stabilization of Earth's surface temperature, J. Geophys. Res. 86, 9776–9782, 1981
18 R.A. Berner, A.C. Lasaga and R.M. Garrels, The carbonate-silicate geochemical cycle and its effect on atmospheric carbon dioxide over the past 100 million years, Am. J. Sci. 283, 641–683, 1983.
19 A C. Lasaga, R.A. Berner and R.M. Garrels, An improved geochemical model of atmospheric CO_2 fluctuations over past 100 million years, in: The Carbon Cycle and Atmospheric CO_2: Natural Variations Archean to Present, E.T. Sundquist and W.S. Broecker, eds, pp 397–411, AGU, Washington, D.C., 1985.
20 P.J McGovern and G Schubert, Thermal evolution of the Earth effects of volatile exchange between atmosphere and interior, Earth Planet. Sci. Lett. 96, 27–37, 1989.
21 G Schubert, D.L. Turcotte, S.C. Solomon and N.H. Sleep, Coupled evolution of the atmospheres and interiors of planets and satellites, in: Origin and Evolution of Planetary and Satellite Atmospheres, S.K. Atreya, J B. Pollack and M S. Matthews, eds., 881 pp, Univ. Arizona Press, Tucson, Ariz., 1989.
22 W.S. Broecker and T.-H. Peng, Tracers in the Sea, 690 pp., Eldigio, 1982.
23 H D Holland, The Chemistry of the Atmosphere and Oceans, 351 pp., Wiley, New York, 1978.
24 T.J. Wolery and N.H. Sleep, Hydrothermal circulation and geochemical flux at mid-ocean ridges, J. Geol. 84, 249–275, 1976.
25 A. Reymer and G. Schubert, Phanerozoic addition rates to the continental crust and crustal growth, Tectonics 3, 63–77, 1984.
26 J F Kasting and T.P. Ackerman, Climatic consequences of very high carbon dioxide level in the Earth's early atmosphere, Science 234, 1383–1385, 1986.
27 J.C.G. Walker, Possible limits on the composition of the Archean ocean, Nature 302, 518–520, 1983.
28 N.H. Sleep, Thermal history and degassing of the Earth: some simple calculations, J. Geol 87, 671–686, 1979.
29 G. Schubert, Subsolidus convection in the mantles of terrestrial planets, Annu. Rev Earth Planet. Sci. 7, 289–342, 1979.
30 G. Schubert, D. Stevenson and P Cassen, Whole planet cooling and the radiogenic heat source contents of the Earth and Moon, J Geophys. Res. 85, 2531–2538, 1980
31 U.R. Christensen, Thermal evolution models for the Earth, J. Geophys. Res. 90, 2995–3007, 1985.
32 P.N Chopra and M.S. Paterson, The role of water in the deformation of dunite, J. Geophys. Res 89, 7861–7876, 1984.
33 R.S.J. Sparks, The dynamics of bubble formation and growth in magmas: A review and analysis, J. Volcanol. Geotherm. Res. 3, 1–37, 1978.
34 Y. Bottinga and M. Javoy, MORB degassing: Bubble growth and ascent, Chem. Geol 81, 255–270, 1990.
35 E. Tajika, Evolution of the atmosphere and ocean of the Earth. Global geochemical cycles of C, H, O, N, and S, and degassing history coupled with thermal history, Thesis, Univ. Tokyo, 1992.
36 DR. Turcotte and G Schubert, Geodynamics, 450 pp., Wiley, New York, 1982.
37 D. Mckenzie and M.J Bickle, The volume and composition of melt generated by extension of the lithosphere, J. Petrol. 29, 625–679, 1988.
38 A. Poldervaart, Chemistry of the Earth's crust, Geol. Soc Am Spec. Pap. 62, 119–144, 1955.
39 J.M. Hunt, Distribution of carbon in crust of the Earth, Bull. Am. Assoc. Pet. Geol. 56, 2273–2277, 1972.
40 A.B Ronov and A.A. Yaroshevsky, A new model for the chemical structure of the Earth's crust, Geokhimiya 12, 1761–1795, 1976
41 B. Marty and A. Jambon, $C/^3He$ in volatile fluxes from the solid Earth· Implications for carbon geodynamics, Earth Planet Sci Lett. 83, 16–26, 1987
42 Y Abe, Abundance of carbon in an impact-induced proto-atmosphere, Proc 21st ISAS Lunar Planet Symp., pp. 238–244, 1988.
43 Y. Abe, Conditions required for formation of ocean water on an Earth-sized planet, in: Lunar Planet Sci. XIX, pp. 1–2, Lunar Planet. Inst., Houston, 1988
44 E Ito, D.M. Harris and A.T. Anderson, Alteration of oceanic crust and geologic cycling of chlorine and water, Geochim Cosmochim. Acta 47, 1613–1624, 1983.
45 C.E. Junge, M. Schidlowski, R. Eichmann and H. Pietrek, Model calculations for the terrestrial carbon cycle: Carbon isotope geochemistry and evolution of photosynthetic oxygen, J. Geophys. Res. 80, 4542–4552, 1975
46 M. Schidlowski, A 3,800-billion-year isotopic record of life from carbon in sedimentary rocks, Nature 333, 313–318, 1988.
47 W.T. Holser, M Schidlowski, F T. Mackenzie and J.B. Maynard, Biogeochemical cycles of carbon and sulfur, in: Chemical Cycles in the Evolution of the Earth, C.B. Gregor, R.M. Garrels, F.T. Mackenzie and J.B. Maynard, eds., pp. 105–174, Wiley, New York, 1988
48 D J Des Marais and J.G. Moore, Carbon and its isotopes in mid-oceanic basaltic glasses, Earth Planet. Sci Lett. 69, 43–57, 1984
49 E. Tajika and T Matsui, Evolution of seafloor spreading rate based on ^{40}Ar degassing history, in prep.
50 D Forsyth and S Uyeda, On the relative importance of the driving forces on plate motion, Geophys. J. R Astron. Soc 43, 163–200, 1975